Ray Tracing Based 60 GHz Channel Clustering and Analysis in Staircase Environment

Ray Tracing Based 60 GHz Channel Clustering and Analysis in Staircase Environment

Yuqian Yang[1], Jian Sun[1,2], Wensheng Zhang[1], Cheng-Xiang Wang[1,3], and Xiaohu Ge[4]
[1]Shandong Provincial Key Lab of Wireless Communication Technologies, Shandong University, Jinan, 250100, China.
[2]State Key Lab. of Millimeter Waves, Southeast University, Nanjing, 210096, P.R.China.
[3]Institute of Sensors, Signals and Systems, School of Engineering & Physical Sciences, Heriot-Watt University, Edinburgh, EH14 4AS, UK.
[4]School of Electronic Information and Communications, Huazhong University of Science and Technology, Wuhuan 430074, Hubei.
Email: yangyuqianworking@126.com, sunjian@sdu.edu.cn, zhangwsh@sdu.edu.cn, cheng-xiang.wang@hw.ac.uk, xhge@mail.hust.edu.cn

***Abstract*—Channel modeling is of vital importance to the development and performance evaluation of wireless communication systems. Though many millimeter-wave (mmWave) channel models have been proposed, few of them concern about staircase environments. This paper analyzes the statistical characteristics of 60 GHz channels in a staircase environment with the transmitter (Tx) side fixed and the receiver (Rx) side moving, especially the variation of characteristics arising from the motion of receiver Rx. Fuzzy c-means (FCM) algorithm is applied in clustering procedure and the Kim-Park (K-P) index combined with the multipath component distance (MCD) are utilized to obtain the optimal cluster number. Simulation results show that almost all of the channel characteristics are related to the Euclidean distance between the Tx and Rx. Also, they are affected by building structures, which will provide guidance on the layout of communication devices.**

***Index Terms*—Ray tracing, mmWave, FCM, K-P index, clustering.**

I. Introduction

The fifth-generation (5G) wireless communication technologies have been proposed and promoted in recent years, and will be commercialized around 2020. Higher frequency bands, known as mmWave frequency bands, are released to support 5G communications. Different from the sub-6 GHz bands, mmWave has its own unique properties, *e.g.*, high path loss and penetration loss, good anti-interference performance, and easily affected by human body movements [1]. When wavelength goes in millimeter scale, the interactions between rays and objects are fairly different from those in lower frequency bands. Considering the above reasons, measuring and analyzing propagation channel characteristics at mmWave frequency bands have become a hot research topic.

Since 60 GHz band has at least 5 GHz bandwidth available worldwide, it is a promising candidate for 5G wireless communication systems [2]. Two IEEE standards on communications at 60 GHz have been finalized in the past decade. IEEE 802.15.3c presents a single-input-multiple-output (SIMO) model which is adoptable for office and conference room scenarios [3]. IEEE 802.11ad is an advanced wireless fidelity (Wi-Fi) standard applicable to three basic scenarios: conference room, enterprise cubicle, and living room [4]. The upcoming IEEE 802.11ay standard, which was proposed as an improvement of 802.11ad, not only adds some new scenarios but also specifies several single-user multiple-input-multiple-output (SU-MIMO) cases for these indoor scenarios [5]. However, none of them covers staircase scenarios.

As a crucial part of indoor environments, a staircase acts as an important role in communication system and may contribute to the organization of 5G cellular networks [6]. Measurement and simulation were conducted in staircase environments at 2.6 GHz [7]–[9]. In [7], a novel path loss model was proposed, introducing the height attenuation factor into the usual local path loss model, making it more practical and flexible. Some small-scale fading parameters were considered in [8]. A discrete tapped delay line (DTDL) power delay profile (PDP) model was presented in [9] to characterize the multipath effect in indoor staircase environments.

So far, many simulation and measurement approaches have been implemented in several typical scenarios at 60 GHz, either indoors or outdoors. In [10], both rotated directional antenna (RDA) method and uniform virtual array (UVA) method were adopted to measure office environments. A wideband channel sounder using RDA method was applied in [11] to analyze the large-scale fading in the campus. The comparison of measurement results and simulation results in the same office environment was shown in [12]. However, little attention has been paid to the channel analysis in staircase scenarios at 60 GHz.

To fill this gap, channel parameters in a staircase environment at 60 GHz are analyzed using ray tracing approach in this paper. Ray tracing is a classical deterministic method used for predicting radio propagation. It is based on the geometrical optic (GO) and uniform of diffraction theory (UTD). The interactions between rays and objects can be classified as reflection, scattering, and diffraction. By tracing paths, all the possible rays can be found. Compared with Shooting and bouncing ray (SBR) method, the image-based method has higher accuracy. However, it is infeasible for diffraction and is fairly time-consuming when reflection times exceeds five. Once the location of the Tx and/or Rx changes, the ray tracing process has to be operated again. SBR method is more widely utilized since it has more simplified calculation process but comparable accuracy. All the simulation results in this paper

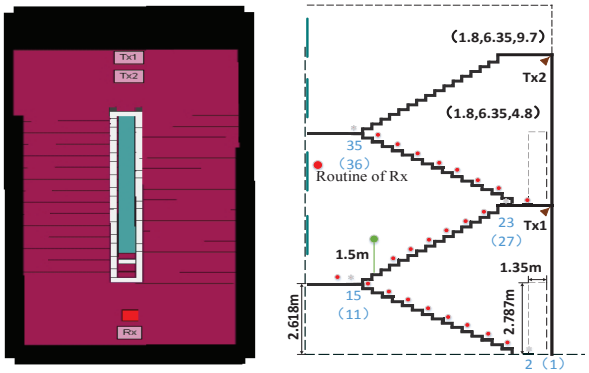

(a) (b)

Fig. 1. (a) Top view of the staircase scenario and (b) layout of the simulation environments.

TABLE I
ELECTROMAGNETIC PARAMETERS OF MATERIALS.

Materials	Permittivity (F/m)	Conductivity (S/m)	Thickness (m)
Concrete	5.31	0.897	0.3 (walls) 0.1 (stairs) 0.1 (floors)
Glass (window)	6.27	0.567	0.01
Metal (handrail and stem)	1	∞	0
Ceiling	1.5	0.0586	0.3

TABLE II
POSITION INDEX REPRESENTATION.

Position index	Behavior	Scenario classification in Tx1/Tx2
1–2	Parallel translation (base floor)	LOS/NLOS
2–11	Walking upstairs (first half floor)	LOS/NLOS
12	Parallel translation (first half floor)	LOS/NLOS
13	Parallel translation (first half floor)	LOS/LOS
14–15	Parallel translation (first half floor)	NLOS/LOS
15–23	Walking upstairs (first floor)	NLOS/LOS
23–27	Parallel translation (first floor)	NLOS/LOS
27–35	Walking upstairs (one and half floors)	NLOS/LOS
35–37	Parallel translation (one and half floors)	NLOS/LOS

are acquired by using Wireless InSite, a commercial software for radio propagation analysis with SBR method.

This paper mainly focuses on the variation of channel characteristics caused by the motion of the Rx. Cluster effect is also put into consideration. Research results may lay impact on the position choice of 60 GHz communication devices.

The reminder of this paper is organized as follows. In Section II, the staircase environment and channel characteristics are illustrated. Section III presents a combined clustering algorithm as well as the cluster parameters. Simulation results and analysis are given in Section IV. Finally, conclusions are drawn in Section V.

II. A STAIRCASE ENVIRONMENT AND CHANNEL CHARACTERISTICS

A. Environment Setup

We chose the first three floors of a staircase in the building of School of Information Science and Engineering, Shandong University, Jinan, China. The simulation environment was set up on the basis of measurement data. Fig. 1(a) is the three-dimensional (3-D) project view realized in Wireless InSite and Fig. 1(b) shows the layout of the scenario. The overall size of the environment is about $3.6\times7.6\times11.931$ m^3. The simulation scenario is assumed to be closed. In other words, a ceiling board is added which does not exist in reality. Each floor contains 16 steps. Each step is 1.62m long, 0.154m high, and 0.54m wide. Walls, floors, and steps are made of concrete, and the handrail is assumed to be made from ideal conduct. There are four windows on one side of the walls. All of them are equipped with metal stems. The electromagnetic parameters of materials obtained from ITU-R P.1238-6 [13] are shown in Table I. To simplify the simulation process, roughness was not put into consideration. The locations of Tx1 and Tx2 are labelled in Fig. 1(b). The Rx is assumed as the mobile station (MS) moving step by step. Isotropic antennas are used at both the Tx and Rx and thus, rays can shoot in all directions with spatial resolution of $2.5°$. The transmit power was set as 0 dBm, and the receive power threshold is -140 dBm. Five reflections, one transmission, and one diffraction have been justified for indoor ray tracing configurations [14].

We set 37 receive points to imitate body movement along the staircase. Table II illustrates the behavior that different position indices represent. For Tx1, Positions 1–13 are line-of-sight (LOS) scenarios and others are non-line-of-sight (NLOS) scenarios. Conversely, for Tx2, Positions 1–12 are in NLOS condition while others are in LOS condition.

B. Channel Model and Statistical Characteristics

The channel model is based on the multipath components (MPCs). The double-directional channel impulse response is given by

$$h(t,\Omega_r,\Omega_t)=\sum_{l=1}^{L}\alpha_l e^{j\varphi_l}\delta(t-\tau_l)\delta(\Omega_r-\Omega_{r,l})\delta(\Omega_t-\Omega_{t,l}). \tag{1}$$

In (1), Θ_l = [α_l, φ_l, τ_l, $\Omega_{r,l}$, $\Omega_{t,l}$] is the parameter vector of the l^{th} MPC, corresponding to the amplitude, phase, delay, angle of arrival (AOA), and angle of departure (AOD), respectively. Here, $\Omega_{t,l}$ represents both elevation angle of departure (EAOD) and azimuth angle of departure (EAOA). Similarly, $\Omega_{r,l}$ represents both elevation angle of arrival (EAOA) and azimuth angle of arrival (AAOA).

Statistical characteristics of wireless channels, including power delay profile (PDP), root mean square (RMS) delay spread (DS), and RMS angle spread (AS), can help evaluate the properties of investigated channels.

1) RMS DS and RMS AS: DS and AS are two typical parameters related to multipath effect. DS and AS indicate the power dispersion in the delay domain and angular domain respectively. RMS DS and RMS AS can be calculated as

$$\sigma_\tau=\sqrt{\frac{\sum_{l=1}^{L}\alpha_l^2\tau_l^2}{\sum_{l=1}^{L}\alpha_l^2}-(\frac{\sum_{l=1}^{L}\alpha_l^2\tau_l}{\sum_{l=1}^{L}\alpha_l^2})^2} \tag{2}$$

$$\sigma_\theta = \sqrt{\frac{\sum_{l=1}^{L} \alpha_l^2 \theta_l^2}{\sum_{l=1}^{L} \alpha_l^2} - (\frac{\sum_{l=1}^{L} \alpha_l^2 \theta_l}{\sum_{l=1}^{L} \alpha_l^2})^2} \quad (3)$$

where θ_l represents either elevation or azimuth AOA.

2) PDP: PDP represents how the received power is distributed in the delay domain and can be expressed as

$$\phi_h(\tau) = \sum_{l=1}^{L} \alpha_l^2 \delta(\tau - \tau_l). \quad (4)$$

When considering the restriction of bandwidth, filtering has to be conducted in the frequency domain. A modified Hanning Window function can be expressed as

$$H(\omega, f_c) = 1.38(\frac{\sin(\omega\tau)}{\omega\tau} + \frac{\sin(\omega\tau + \pi)}{\omega\tau + \pi} + \frac{\sin(\omega\tau - \pi)}{\omega\tau - \pi})e^{jf_c} \quad (5)$$

where ω and f_c are the bandwidth and carrier frequency of window function, respectively. This modified Hanning window function will be transformed into its time domain version and applied in (4).

III. Cluster Based Channel Model and Parameters

A. Clustering Algorithm

Some of the MPCs having similar delays, AOAs, or AODs can be grouped together and regarded as one cluster. Clustering of MPCs may significantly affect the channel capacity [15] and it will simplify the expression of channel models. Many of the current mmWave channel models are based on the clustering results.

For clustering algorithms, the most frequently used one is K-means algorithm [16]. In this algorithm, the cluster centers are placed as barycenters far away from each other. Nevertheless, the clustering result can be easily influenced by the choice of initial cluster centers, thus the clustering results are not always globally optimized. FCM algorithm [17] is used to avoid this problem in this paper as the cluster centers are determined by the solution of a convex function. The experiment results show that this algorithm can always obtain the global optima. Both clustering algorithms aforementioned need to set the cluster numbers initially. Therefore, it is necessary to determine the optimal number of clusters.

To validate the number of clusters, K-P index is usually utilized [18]. This method uses two functions to define inter- and intra-cluster distances, corresponding to over- and under-partition metrics, respectively. Different from the original K-means algorithm, MCD [19] is applied to measure the distance of two rays as it not only considers both AOA and AOD in the angular domain but also fairly measures angle and time components using weighted normalization. The intra-cluster distance is defined as

$$MCD_k = \frac{1}{n_k} \sum_{j, \Theta_j \in \Phi_k} MCD_{kj} \quad (6)$$

where Θ_j is the parameter vector of the j^{th} ray in the k^{th} cluster, n_k is the ray number of the k^{th} cluster, and Φ_k is the data set of the k^{th} cluster. The MCD metric is calculated as

$$MCD_{ij} = \sqrt{\|MCD_{AOD,ij}\|^2 + \|MCD_{AOA,ij}\|^2 + \|MCD_{\tau,ij}\|^2}. \quad (7)$$

The MCD of delay is given by

$$MCD_{\tau,ij} = \xi \frac{|\tau_i - \tau_j| \tau_{std}}{(\Delta\tau_{max})^2} \quad (8)$$

where $\Delta\tau_{max} = max|\tau_i - \tau_j|$. τ_{std} is the standard deviation of the delays, and ξ is the weight of the time distance compared to the angular distance. In this paper, $\xi = 3$ is confirmed as appropriate.

The distance in angle domain is given by $\|MCD_{AOD/AOA,ij}\| = \frac{1}{2}\|\mathbf{a}_i - \mathbf{a}_j\|_2$, where

$$\mathbf{a}_{i/j} = [\sin\theta_{i/j}\cos\phi_{i/j}, \sin\theta_{i/j}\sin\phi_{i/j}, \cos\theta_{i/j}]^T. \quad (9)$$

In (9), θ_i and ϕ_i refer to the elevation angle and azimuth angle, respectively.

Similarly, the inter-cluster distance function is defined as

$$d_{min} = \min_{c_m \neq c_n} MCD_{mn}, \quad c_m, c_n \in \mathbf{v}. \quad (10)$$

Here, $\mathbf{v}$ is the assembly of cluster center parameter vectors.

Let $\mathbf{X} = [\Theta_1, \Theta_2, \Theta_3, ...\Theta_L]^T$ be the whole set of rays' parameter vectors and $\mathbf{V} = [\mathbf{v}_1, \mathbf{v}_2, \mathbf{v}_3, ...\mathbf{v}_K]^T$ be the set of cluster center parameter vectors. We use $v_u(c, \mathbf{V}; \mathbf{X})$ to represent the under-partition status, *i.e.*,

$$v_u(c, \mathbf{V}; \mathbf{X}) = \frac{1}{c} \sum_{k=1}^{c} MCD_k, \quad 2 \leq c \leq c_{max}. \quad (11)$$

On the contrary, the over-partition metric is given by

$$v_o(c, \mathbf{V}) = \frac{c}{d_{min}}, \quad 2 \leq c \leq c_{max}. \quad (12)$$

The normalization is operated on $v_u(c, \mathbf{V}; \mathbf{X})$ and $v_o(c, \mathbf{V})$ for consistency [18], and the optimal cluster number can be obtained by minimizing

$$u_{SV}(c, \mathbf{V}; \mathbf{X}) = v_{uN}(c, \mathbf{V}; \mathbf{X}) + v_{oN}(c, \mathbf{V}). \quad (13)$$

B. Cluster Parameters

There are five main parameters describing the clustering characteristics, i.e., the cluster arrival rate Λ, ray arrival rate λ, standard deviation of lognormal fading σ, cluster decay factor Γ, and ray decay factor γ. The methodology for computation was detailed in [20]. In order to estimate Λ, the delay of the first arrival ray in each cluster was selected and the forward delay difference is calculated, so that the cluster arrival time follows the exponential distribution as

$$p(T_K|T_{K-1}) = \Lambda \exp(-\Lambda(T_K|T_{K-1})). \quad (14)$$

The ray arrival rate is estimated in a similar way and its value is based on the separation time of adjacent rays. The standard deviation can be obtained by linear fitting of the path loss in logarithmic terms.

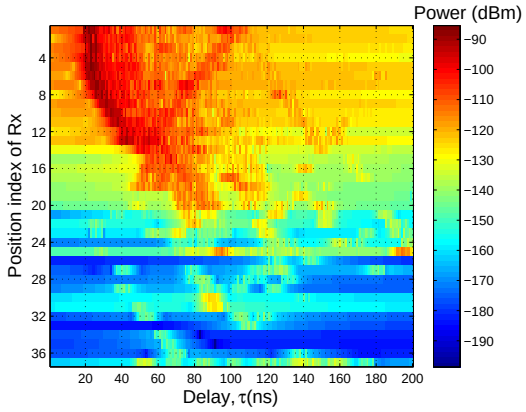

(a)

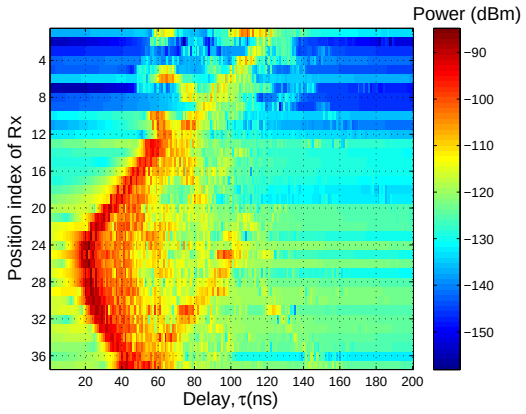

(b)

Fig. 2. (a) PDP of Tx1 and (b) PDP of Tx2.

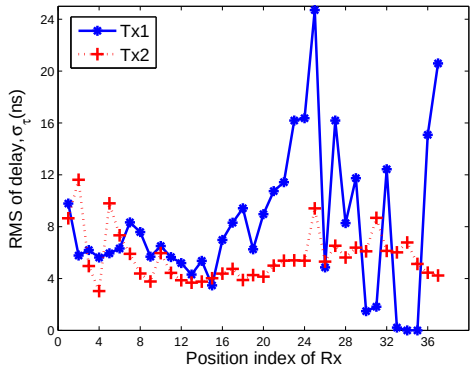

Fig. 3. DS variation with the movement of the Rx.

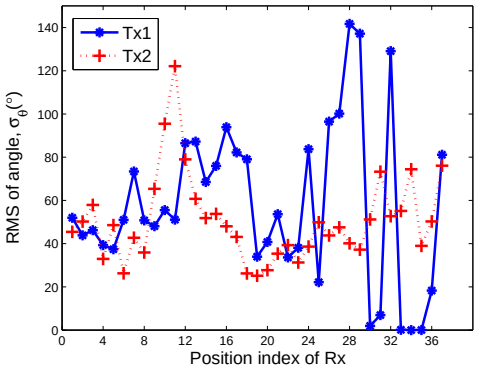

Fig. 4. AS variation with the movement of the Rx.

IV. Ray Tracing Simulation and Analysis

Fig. 2 shows the PDP of Tx1 and Tx2. It is clear that when the distance of the Tx and Rx increases, the delay gets larger and the relative power tends to be lower. In Fig. 2(a), the power decreases sharply after Position 23. Due to the structure of the staircase, when Rx is in Position 23, only few of rays can reach here through high-order reflections and diffractions. The received powers in Positions 23–37 are fairly smaller than those in Positions 1–22.

The RMS DS and RMS AS are presented in Fig. 3 and Fig. 4, respectively. Both of them clarify that when Tx–Rx link is in the LOS condition, the RMS DS and RMS AS remain nearly unchanged, while in the NLOS condition, their values fluctuate intensively. In other words, the communication quality is good and stationary when the sight between the Tx and Rx is unblocked. Once the Rx is sheltered, the connection quality will get ruined.

Comparing the results of Tx1 and Tx2, the received power of Rx–Tx2 link is much higher and the fluctuations of RMS DS and RMS AS of Rx–Tx2 are more smooth despite the Rx is in the NLOS condition. Since Tx2 is placed much higher than Tx1, several reflected rays can reach the Rx without diffraction. The power of these rays is relatively large so that the power dispersion of Rx–Tx2 link is lower than that of Rx–Tx1 link.

From the analyses above, it is necessary to put transmit device on each floor to maintain the communication quality and the device should be placed as high as possible to avoid sheltering.

According to the clustering algorithm introduced above, the number of clusters was counted and the results are illustrated in Fig. 5. Note that those clusters whose power is 40 dB lower than the power of the LOS component in the LOS condition or the power of the strongest cluster in the NLOS condition should be neglected since they have little contribution to the Rx. The clustering results are influenced by surrounding building structures of the Rx. The breaks always occur as the Rx changes its condition. For instance, in terms of Tx1, when MS moves from position 11 to 15, the scenario of MS transfers from LOS to NLOS, and the cluster number decreases since parts of the building are blocked by walls.

Table III and Table IV demonstrate the standard deviations of path loss of Tx1 and Tx2, respectively. They are classified corresponding to the different scenario classes. Results show that the standard deviation is mainly affected by direct and

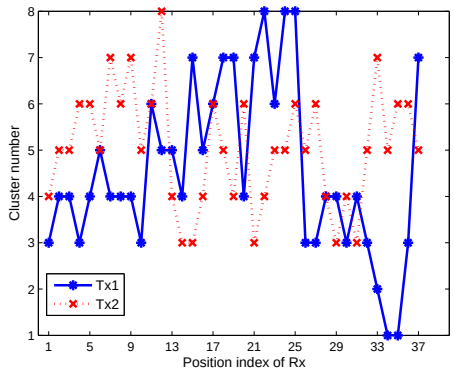

Fig. 5. Cluster number variation with the movement of the Rx.

TABLE III
STANDARD DEVIATION OF LOGNORMAL FADING OF TX1.

Position index	Scenario classification	Standard deviation
1–13	LOS	0.3607
14–23	NLOS (reflection in domination)	3.6498
24–37	NLOS (diffraction in domination)	0.9026
1–37	Overall	1.8383

TABLE IV
STANDARD DEVIATION OF LOGNORMAL FADING OF TX2.

Position index	Scenario classification	Standard deviation
1–12	NLOS	−0.725
13–25	LOS (close to Tx2)	−1.1065
26–37	LOS (away from Tx2)	1.2776

reflected rays.

V. CONCLUSIONS

In this paper, a staircase environment has been set up at 60 GHz and some statistical characteristics have been used to analyze the results of ray tracing. According to the simulation results, it is reasonable to place the transmit device in a higher position of each floor to get better communication performance. A FCM clustering algorithm combined with MCD metric has been proposed. Some of the cluster parameters have been estimated based on the clustering results. As the simulation scenario is specified, all the results may have some limitations. In the future, more simulations and measurements will be carried out to search for a generalized channel model in staircase environments in mmWave bands.

ACKNOWLEDGMENT

The authors gratefully acknowledge the support from the EU RISE TESTBED project (No. 734325), the EU FP7 QUICK project (No. PIRSES-GA-2013-612652), the EU H2020 5G Wireless project (NO. 641985), Natural Science Foundation of China (No. 61210002 ,61771293 and 61371110), and Key R&D Program of Shandong Province (No. 2016GGX101014).

REFERENCES

[1] P. B. Papazian, C. Gentile, K. A. Remley, and Nada Golmie, "A radio Channel Sounder for mobile millimeter-wave communications: system implementation and measurement assessment," *IEEE Trans. Mircow Theory Techni.*, vol. 64, no. 9, pp. 2924–2932, Sept. 2016.

[2] C. Gustafson, K. Haneda, S. Wyne, and F. Tufvesson, "On mm-Wave multipath clustering and channel modeling," *IEEE Trans. Antennas Propag.*, vol. 62, no. 3, pp. 1445–1455, Mar. 2014.

[3] IEEE Standard for Information technology - Telecommunications and information exchange between systems - Local and metropolitan area networks - Specific requirements. Part 15.3: Wireless Medium Access Control (MAC) and Physical Layer (PHY) Specifications for High Rate Wireless Personal Area Networks (WPANs) Amendment 2: Millimeterwave-based Alternative Physical Layer Extension, IEEE Std 802.15.3c-2009 (Amendment to IEEE Std 802.15.3-2003), Oct. 2009.

[4] A. Maltsev *et al.*, *Channel models for 60 GHz WLAN Systems,* IEEE Standard 802.11–09/0334r8, May. 2010.

[5] A. Maltsev, A. Pudeyev, A. Lomayev and I. Bolotin, "Channel modeling in the next generation mmWave Wi-Fi: IEEE 802.11ay standard," in *Proc.European Wireles Conference'16*, Oulu, Finland, May. 2016, pp. 1–8.

[6] X. Ge, S. Tu, G. Mao, C.-X. Wang and T. Han, "5G Ultra-Dense Cellular Networks," *IEEE Wireless Communications*, Vol. 23, No. 1, pp. 72-79, Feb. 2016.

[7] Y. Liu, Y. Yu, W. J. Lu, and H. Zhu, "Antenna-height-dependent path loss model and shadowing characteristics under indoor stair environment at 2.6GHz," *IEEJ Trans. Electrical*, vol. 10, no. 5, pp. 498–502, June. 2015.

[8] Y. Liu, Y. Yu, W. J. Lu, and H. Zhu, "Propagation model and channel simulator under indoor stair environment for machine-to-machine applications," in *Proc. APMC'15*, Nanjing, China, Dec. 2015, pp. 1–3.

[9] Y. Yu, Y. Liu, W. J. Lu, S. Jin, and H. Zhu, "Modelling and simulation of channel power delay profile under indoor stair environment," *IET Commun.*, vol. 11, no. 1, pp. 119–126, Dec. 2016.

[10] X. Wu, C.-X. Wang, J. Sun, J. Huang, R. Feng, Y. Yang, and X. Ge, "60 GHz millimeter-wave channel measurements and modeling for indoor office environment," *IEEE Trans. Antennas Propag.*, vol. 65, no. 4, pp. 1912–1924, Feb. 2017.

[11] E. Ben-Dor, T. S. Rappaport, Y. Qiao, and S. J. Lauffenburger, "Millimeter-wave 60 GHz outdoor and vehicle AoA propagation measurements using a broadband channel sounder," in *Proc. GlobeCom'11*, Huston, USA, Dec. 2011, pp. 5–9.

[12] B. Neekzad, K. Sayrafian-Pour, J. Perez, and J. S. Baras, "Comparison of ray tracing simulations and millimeter wave channel sounding measurements," in *Proc. PIMRC'07*, Athens, Greece, Sept. 2007, pp. 1–5.

[13] International Telecommunication Union, ITU-R, P. 1238–6, "Propagation data and prediction methods for the planning of indoor radio communication systems and radio local area networks in the frequency range 900 MHz to 100 GHz," Oct. 2009.

[14] G. E. Athanasiadou, A. R. Nix and J. P. McGeehan, "A ray tracing algorithm for microcellular and indoor propagation modelling," in *Proc. ICAP'95*, Eindhoven, Netherlands, Apr. 1995, pp. 231–235.

[15] C.-C. Chong, C.-M. Tan, D. I. Laurenson, S. McLaughlin, M. A. Beach, and A. R. Nix, "A new statistical wideband spatio-temporal channel model for 5 GHz band WLAN system," in *IEEE J. Sel. Areas Commun.*, vol. 21, no. 2, pp. 139–150, Apr. 2003.

[16] D. Ganguly, S. Mukherjee, S. Naskar, and P. Mukherjee, "A novel approach for determination of optimal number of cluster," in *Proc. ICCAE'09*, Bangkok, Thailand, Mar. 2009, pp. 113–117.

[17] S. Araki, H. Nomura, and N. Wakami, "Segmentation of thermal images using the fuzzy c-means algorithm," in *Proc. FUZZY'93*, San Francisco, California, Apr. 1993, pp. 719–724.

[18] D. Kim, Y. Park, and D. Park, "A novel validity index for determination of the optimal number of clusters," *IEICE Trans. Inf and Syst.*, vol. E84-D, no. 2, pp. 281–285, Feb. 2001.

[19] N. Czink, P. Cera, J. Salo, E. Bonek, J. P. Nuutinen, and J. Ylitalo, "Improving clustering performance using multipath component distance," *IEEE Electron. Lett.*, vol. 42, no. 1, pp. 33–45, Jan. 2006.

[20] Q. H. Spencer, B. D. Jeffs, M. A. Jensen, and A. L. Swindlehurst, "Modeling the statistical time and angle of arrival characteristics of an indoor multipath channel," in *IEEE J. Sel. Areas Commun.*, vol. 18, no. 3, pp. 347–360, Mar. 2000.